**Smart Structures and Systems**, *Vol. 17, No. 1 (2016) 45-58*
DOI: http://dx.doi.org/10.12989/sss.2016.17.1.045 

# Evaluation of freezing and thawing damage of concrete using a nonlinear ultrasonic method

Hong Jae Yim[1a], Sun-Jong Park[2b], Jae Hong Kim[3c] and Hyo-Gyong Kwak[*2]

*[1]Department of Construction and Disaster Prevention Engineering, Kyungpook National University, 2559 Gyeongsang-daero, Sangju, Gyeongsangbuk-do, 742-711, Korea*
*[2]Department of Civil Engineering, Korean Advanced Institute for Science and Technology, 291 Daehak-ro, Yuseong-gu, Daejeon 305-701, Korea*
*[3]School of Urban and Environmental Engineering, Ulsan National Institute of Science and Technology, Ulsan 698-798, Korea*

*(Received January 28, 2014, Revised August 26, 2014, Accepted September 29, 2014)*

**Abstract.** Freezing and thawing cycles induce deterioration and strength degradation of concrete structures. This study presumes that a large quantity of contact-type defects develop due to the freezing and thawing cycles of concrete and evaluates the degree of defects based on a nonlinearity parameter. The nonlinearity parameter was obtained by an impact-modulation technique, one of the nonlinear ultrasonic methods. It is then used as an indicator of the degree of contact-type defects. Five types of damaged samples were fabricated according to different freezing and thawing cycles, and the occurrence of opening or cracks on a micro-scale was visually verified via scanning electron microscopy. Dynamic modulus and wave velocity were also measured for a sensitivity comparison with the obtained nonlinearity parameter. The possibility of evaluating strength degradation was also investigated based on a simple correlation of the experimental results.

**Keywords:** concrete; freezing and thawing; nonlinear ultrasonic method; contact-type defect

## 1. Introduction

In cold areas freezing and thawing (F-T) repetition leads to deterioration and strength degradation of concrete structures. The concrete damage due to F-T cycles mostly occurs due to freezing of water in capillary pores. When ice formation initiates in capillary pores, the surrounding water migrates to the location of the freezing nucleus. This phenomenon can be explained by an osmotic effect and vapor pressure difference between the ice and supercooled water (Mindess *et al.* 2003). The capillary pores then continue to fill with ice, which leads to volume expansion of the pores. From reiterated F-T cycles, progressive expansion of the cement paste causes internal damage of the cement paste matrix due to its tensile failure (Mehta and

∗Corresponding author, Professor, E-mail: khg@kaist.ac.kr
[a] Assistant Professor, E-mail: yimhongjae@gmail.com
[b] Ph.D. Student, E-mail: battlemarine@kaist.ac.kr
[c] Associate Professor, E-mail: jhk3001@gmail.com


http://www.techno-press.org/?journal=sss&subpage=8 ISSN: 1738-1584 (Print), 1738-1991 (Online)

Monteiro 2006). This study presumes that the damage by accumulated F-T cycles is contact-type defects including opening by tensile failure and consequent multi-scale cracks, and attempts to assess the degree of F-T damage using an ultrasonic wave technique.

Various ultrasonic techniques have been developed for nondestructive evaluation of damaged cement-based materials (Popovics *et al.* 1990, ACI Committee 228 1998, Selleck *et al.* 1998, Kim and Kwak 2008, Kim *et al.* 2010, Yim *et al.* 2012b). Among them, the measurement of dynamic elastic modulus has been introduced and widely used to relatively represent the deteriorated condition of concrete according to the reiterated F-T cycles (ASTM C 666-03 2008). Wave velocity measurement is also applied for F-T damage evaluation (Selleck *et al.* 1998). Previous studies using both techniques to evaluate F-T damage on normal or high strength concrete have been reported (Jacobsen *et al.* 1995, Jacobsen and Sellevold 1996), and water transport characteristics of F-T damaged concrete have been identified (Yang *et al.* 2006). Ultrasonic images of F-T damaged concrete have more recently been generated (Molero *et al.* 2012).

While results of linear acoustic methods can reflect the material properties of the medium, it is difficult to represent the degree of distributed and cumulated damage in a multi-scale. In particular, their sensitivity to damage is less than that obtained by a nonlinear acoustic method (Nagy 1998, Yim *et al.* 2012a). Nonlinear acoustic methods were applied to fatigue damage or early crack detection in metal materials (Nagy 1998, Herrmann *et al.* 2006, Zaitsev *et al.* 2006), where the crack was a contact-type defect involving opening and closing at the level of the applied stress wave. During the hardening of cement-based materials, contact-type defects inherently occur in the medium. In addition, large amounts of contact-type defects lead to degradation and nonlinear behavior of concrete. Accordingly, the nonlinear ultrasonic technique is efficient for nondestructive evaluation of contact-type defect in cement-based materials. Its application includes evaluating the strength of concrete (Warnemuende and Wu 2004), damage due to alkali-silica reaction (Chen *et al.* 2008), and water saturation effects (Payan *et al.* 2010a). Recently, thermal damage of concrete was also evaluated using a nonlinear ultrasonic technique (Yim *et al.* 2012a).

Accumulated F-T cycles generate additional contact-type defects in concrete. Nevertheless, F-T damage has not been investigated to date using a nonlinear ultrasonic technique. This study attempts to evaluate F-T damaged concrete by application of a nonlinear ultrasonic technique, and identifies that contact-type defect is one of the major symptom by F-T damage. For this purpose, concrete samples on five types of damage were damaged according to different reiterated F-T cycles, and an optical investigation of enhanced opening or cracks was performed using a scanning electron microscope (SEM). The nonlinearity parameter for each sample was measured by an impact-modulation nonlinear ultrasonic technique. Conventional methods, such as measurement of the dynamic modulus or wave velocity, were also applied on the damaged samples for comparison of sensitivity with the results of the nonlinearity parameter. In addition, compressive strengths of the samples were obtained and their degradation was correlated with the increased ratio of the nonlinearity parameter to investigate the possibility of strength evaluation using the nonlinear ultrasonic technique.

## 2. Concrete samples

A total of 15 cylindrical concrete samples (Φ100×200 mm) were prepared, and the mix proportion is given in Table 1. The water-to-cement weight ratio and fine-to-coarse aggregate weight ratio of the mixture was 0.5 and 0.68, respectively. Type I Portland cement was used. No admixture was added during mixing. River sand and crushed gravel having maximum size of 5 mm and 19 mm, respectively, were used as fine and coarse aggregate. After three months of curing in water, the samples were subjected to F-T cycles. According to the repetition of F-T cycles, the samples were classified into five groups, labeled C00, C10, C30, C50, and C70, which correspond to the intact case (0 cycle), 10 cycles, 30 cycles, 50 cycles, and 70 cycles, respectively. Table 2 shows the density and apparent expansion of samples at room temperature (22˚C). The apparent expansion is the volume increase during F-T cycles, which is obtained by dimensional measurement. The results were averaged with three samples, where dimensional measurements of each sample were performed 10 times at different locations. Prior to F-T cycles, the concrete samples were placed in a water bath and then immediately moved to the F-T testing machine. The samples were thus fully saturated and subjected to accelerated F-T cycles in accordance with procedure B introduced in ASTM C-666 (ASTM C 666-03 2008). All samples were completely surrounded by air during the freezing cycle and submerged in water during the thawing cycle. Fig. 1 shows a typical temperature change during the F-T cycles. The period of a F-T cycle was 120 min: the freezing phase was about 90 min and the thawing phase was 30 min. The lowest and highest temperature of the F-T cycles was -16˚C and 5˚C, respectively.

Table 1 Mix proportion of concrete (kg/m$^3$)

| Water | Cement | Fine aggregate | Coarse aggregate | Water-to-cement ratio | Fine-to-coarse aggregate ratio |
|---|---|---|---|---|---|
| 160 | 320 | 744 | 1100 | 0.5 | 0.68 |

Table 2 Material properties of concrete samples

| Label | Density (kg/m$^3$) | Apparent expansion (%) |
|---|---|---|
| C00 | 2400 | - |
| C10 | 2407 | 0.054 |
| C30 | 2419 | 0.046 |
| C50 | 2420 | 0.079 |
| C70 | 2409 | 0.092 |

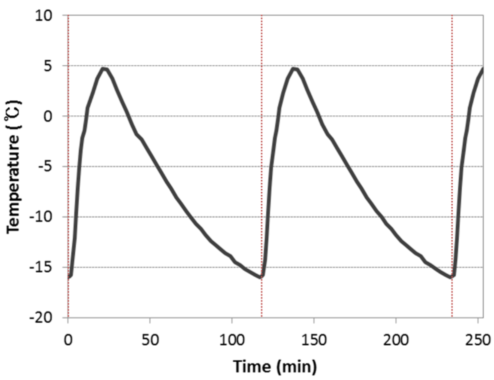


Fig. 1 Freezing and thawing cycles

## 3. Nonlinear ultrasonic method

Heterogeneous materials including concrete present hysteresis and discrete memory in their stress-strain relation. However, the mechanism of the nonlinear response is not completely understood yet. Researchers have investigated the nonlinear response upon stress wave propagation in cement-based materials (Buck *et al.* 1978, Antonets *et al.* 1986, Van Den Abeele 1996, Payan *et al.* 2010b, Yim *et al.* 2012a, Yim *et al.* 2014). Waves are propagated through heterogeneous materials, which have a nonlinear acoustic response, and this phenomenon is more pronounced with an increase of material nonlinearity. The constitutive law for the phenomenon introduces nonlinear parameters as follows (Hikata *et al.* 1963, Van Den Abeele 1996, Van Den Abeele *et al.* 2000, Van Den Abeele *et al.* 2001)

$$\sigma = E_0\varepsilon(1+\beta\varepsilon+\gamma\varepsilon^2)+h\left\{\varepsilon, \mathrm{sign}(\dot{\varepsilon})\right\} \tag{1}$$

where $\sigma$ is stress, $E_0$ is Young's modulus representing the linear response of a material, $\varepsilon$ is strain, $\beta$ and $\gamma$ are the classical nonlinear perturbation coefficients in the Taylor expansion of stress-strain relationship, $h$ is a nonlinear hysteric function, and $\dot{\varepsilon}$ is the rate of strain ($d\varepsilon/dt$). The *sign* function is +1 if $\dot{\varepsilon} > 0$ and −1 if $\dot{\varepsilon} < 0$. When a wave propagates through a material governed by the foregoing constitutive nonlinear equation, the nonlinear acoustic responses show a higher harmonic or sub-harmonic mode, mixed frequency response, or a shift of the resonance frequency (Jhang 2009). In this study the mixed frequency response was measured by an impact-modulation spectroscopy method to evaluate the F-T damage of concrete samples. This method was introduced to generate a high frequency signal through sinusoidal ultrasonic waves produced by the through-transmission method, and low frequency vibration by resonance of the samples using an impact hammer (Yim *et al.* 2012a, Yim *et al*. 2014).

## 4. Experiments via impact-modulation technique

Fig. 2 shows the experimental setup for impact-modulation measurement of the concrete samples. An impact hammer (086C03; PCB Piezotronics, Inc.) and ultrasonic longitudinal narrow-band transducers (Panametrics X1019; Olympus NDT, Inc.) were used to simultaneously generate resonant vibration of the sample and a sinusoidal continuous signal. Two transducers were located at the sample side and impact vibration was generated at the center of the sample. The nominal center frequency of the transducers and the frequency of the propagating ultrasonic wave is about 46.1 kHz. A high frequency ultrasonic wave was generated and amplified with the use of a function generator (NI PXI-5421; National Instruments Corp.) and a power amplifier (BA4825; NF Corp.). The measured signal was digitized using an analogue-to-digital converter (NI PXI-5105; National Instruments Corp.) at an 80 MS/s sampling rate and 12 bit resolution. Low frequency vibration generated by the impact hammer was measured via a triaxial accelerometer (356A33; PCB Piezotronics, Inc.) at the opposite side of the impact location and digitized using an analogue-to-digital converter (NI PXI-4472B; National Instruments Corp.) at a 102.4 kS/s sampling rate and 24 bit resolution. The mixed signal was recorded for 0.2 sec, and zero padding of 0.8 sec was added to improve frequency resolution in the transformed spectrum. A Hann window of 1 sec was also applied to isolate the main response. Low-frequency vibration ($f_0$) and an ultrasonic wave of high frequency ($f_1$) were generated simultaneously. High and low frequencies can be classified by their relative difference. In this study, an ultrasonic wave and vibration by impact were used as high and low frequency, respectively. Opening and closing of contact-type defects in concrete induces modulation of the mixed waves having different frequencies, which results in modulated spectra in the area around the high frequency wave. These frequency-modulated components are located at the sideband ($f_1 \pm f_0$), and the modulated spectra can reflect the degree of opening and closing at contact-type defects. As a result, the degree of F-T defects is represented by the nonlinearity parameter ($D$). The value of the nonlinearity parameter can be calculated by the spectral energies of the generated frequencies as follows (Donskoy *et al.* 2001, Warnemuende and Wu 2004, Yim *et al.* 2012a)

$$\frac{E_s}{E_h} \propto DE_l \qquad (2)$$

where $E_h$, $E_l$, and $E_s$ are the spectral energy of a high frequency wave, low frequency vibration, and the sideband component, respectively. Spectra of low frequency vibration are distributed below 5 kHz, and therefore the spectral energy for vibration ($E_l$) was integrated up to a power spectral density of 5 kHz. Representative spectra of low frequency vibration are shown in Fig. 3(a). The modulated sidebands were also designated from 41.1 kHz to 51.1 kHz excluding the range of 46 kHz to 46.2 kHz, where the spectral energy of the high frequency wave distributes. Magnified representative spectra of modulated high frequency waves of intact and damaged samples are presented in Fig. 3(b), where the spectral densities are calculated via a fast Fourier transform. To evaluate the nonlinearity parameter, the tests were performed by varying the spectral energy of low frequency vibration, while maintaining the spectral energy of a high frequency wave as constant. As can be seen in the comparative results, the spectral density of the intact sample (no F-T history) has no modulated component on the sideband, but the damaged samples (50 F-T cycles) have several peaks in the modulated spectra on the sideband.

Fig. 4(a) shows the results of spectral energies and their linear trend according to accelerated F-T cycles. A total of 20 measurements for each sample are plotted as a curve representing the relationship of the modulated energy ($E_s/E_h$) and the impact vibration ($E_l$).

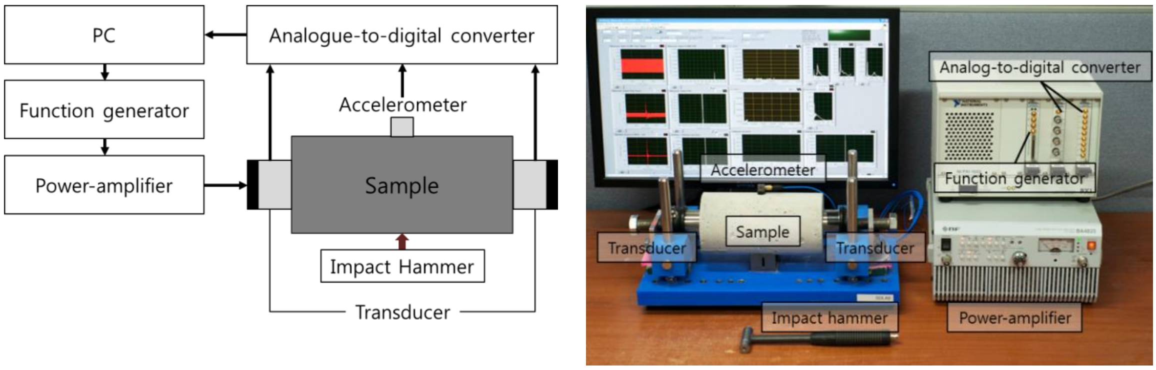


(a) Experimental setup (b) Schematic apparatus of experimental system

Fig. 2 Impact-modulation experiment

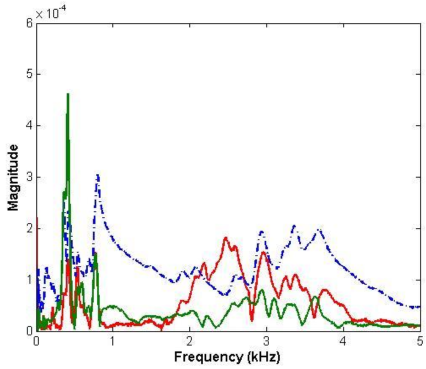


(a)

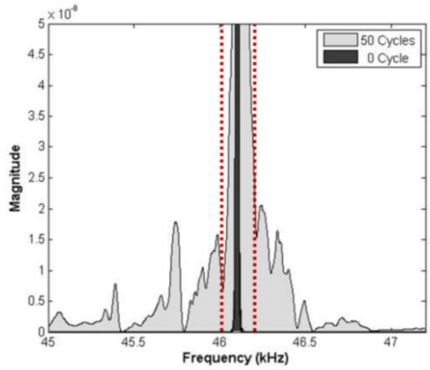


(b)

Fig. 3 The frequency spectra: (a) the low frequency vibration freezing and thawing for 50 cycles and (b) the modulated high frequency wave freezing and thawing for 50 cycles and an intact sample (0 cycle)

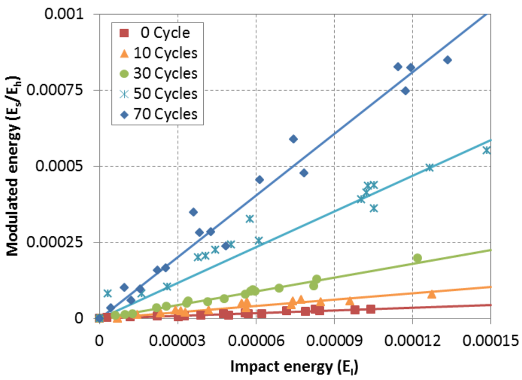


(a)

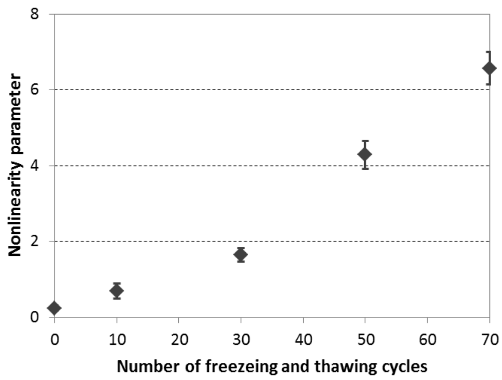


(b)

Fig. 4 (a) Spectral energies of concrete samples and (b) the averaged nonlinearity parameters according to number of freezing and thawing cycles

Table 3 Results of conventional and nonlinear ultrasonic methods on F-T damaged samples

| Label | Nonlinearity parameter | Wave velocity (km/s) | Dynamic modulus (GPa) |
|---|---|---|---|
| C00 | 0.239 | 4.307 | 42.00 |
| C10 | 0.698 | 4.208 | 38.14 |
| C30 | 1.647 | 4.094 | 34.96 |
| C50 | 4.290 | 3.399 | 27.80 |
| C70 | 6.574 | 3.390 | 22.55 |

Fig. 5 Polymer molds incorporating concrete samples for SEM analysis

The variation of the results is caused by the impact power and modulation of the wave. The slope of each linear trend is the nonlinearity parameter ($D$) to be determined. Fig. 4(b) is the averaged nonlinearity parameters of 3 samples, where 5 independent measurements were performed at different locations of each sample. The variation of 15 nonlinearity parameters under different F-T cycles is also plotted to show the sensitivity of the impact-modulation technique. The obtained nonlinearity parameters are listed in Table 3. The obtained nonlinearity parameters increased with accumulated F-T cycles. Based on the experimental measurements, it can be concluded that the contact-type defects meaningfully accounted for F-T damage and their degree can be evaluated by the impact-modulation technique. Optical investigation using SEM was subsequently carried out to support that F-T damage mainly consists of contact-type defects.

## 5. SEM for F-T damaged samples

As can be seen from the apparent expansion results listed in Table 2, all samples expanded less than 0.1%. Iterated F-T cycles induce internal defects and then cause expansion of the samples. The internal defects were visualized at the micro-scale for each group of samples. For SEM images, a small piece of concrete sample was removed and prepared through two steps, polymer mounting and polishing. After being subjected to F-T cycles, all samples were dried at 60˚C for 2 days and embedded in a low-viscosity polymer. The polymer solidifies for 2 days at room temperature (22˚C) and the polymer mounting prevents additional mechanical cracking caused by successive polishing. Fig. 5 shows 10 polymer-mounted samples ($\Phi32\times15$ mm). The samples were subsequently polished using a rapping wheel with finer silicon carbide abrasive paper in the order of #400, #800, #1500, #2000, and #4000. Drying the samples in a 75˚C oven was followed to remove pore water, which is helpful for maintaining a vacuum condition in the SEM instrument. A prepared sample was attached on a steel stub using carbon tape and silver paste, and its upper surface was then coated with gold paste to avoid buildup of electrons. The specimens were observed via back-scattered electron imaging with SEM, which is effective for micro-scale morphology analysis (Stutzman 2004).

Figs. 6 to 8 show SEM micrographs of an intact sample (0 cycle) and F-T damaged samples (30 or 50 F-T cycles) with magnification of 150, 500, 10,000, and 40,000 times. In the SEM images in the figures, cavities (voids or openings) are represented as a relatively dark color, and are mainly located at the interfaces between constituents. The amount (area) of these defects was visibly enhanced with accumulated F-T cycles, as expected, and significant amounts of defects can be observed in locations around aggregates (where an interfacial transition zone is located). However, no morphological change such as plastic deformation or collapse of hydrated phases was observed in the investigated samples. Accordingly, it is concluded that iterated F-T cycles mainly create contact-type defects at a micro-scale.

## 6. Discussion

In order to investigate the efficiency of the impact-modulation technique for evaluating F-T damage, the results were compared with those obtained by conventional techniques (linear ultrasonic or vibration testing). Measurement of the dynamic modulus and wave velocity was conducted. The dynamic modulus of elasticity can be easily determined by measuring the resonant frequency of longitudinal impact-induced vibration (ASTM C 215-08 2008).

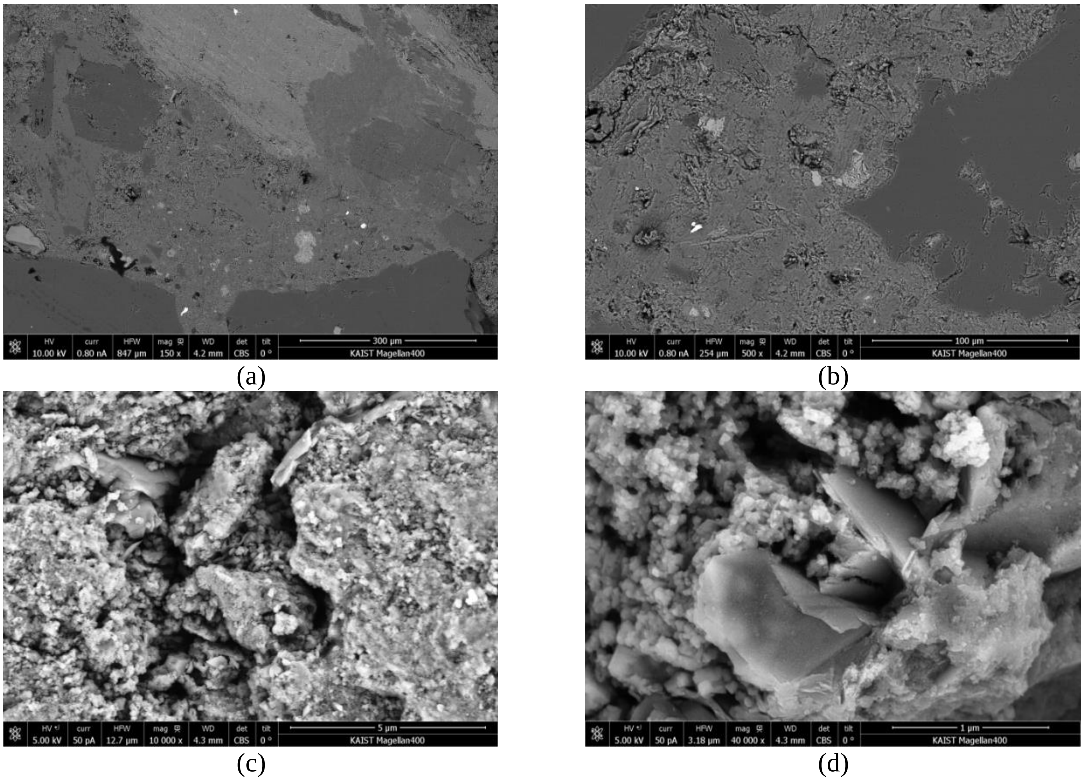

Fig. 6 SEM micrographs of intact sample with magnification of (a) 150 times, (b) 500 times, (c) 10,000 times and (d) 40,000 times

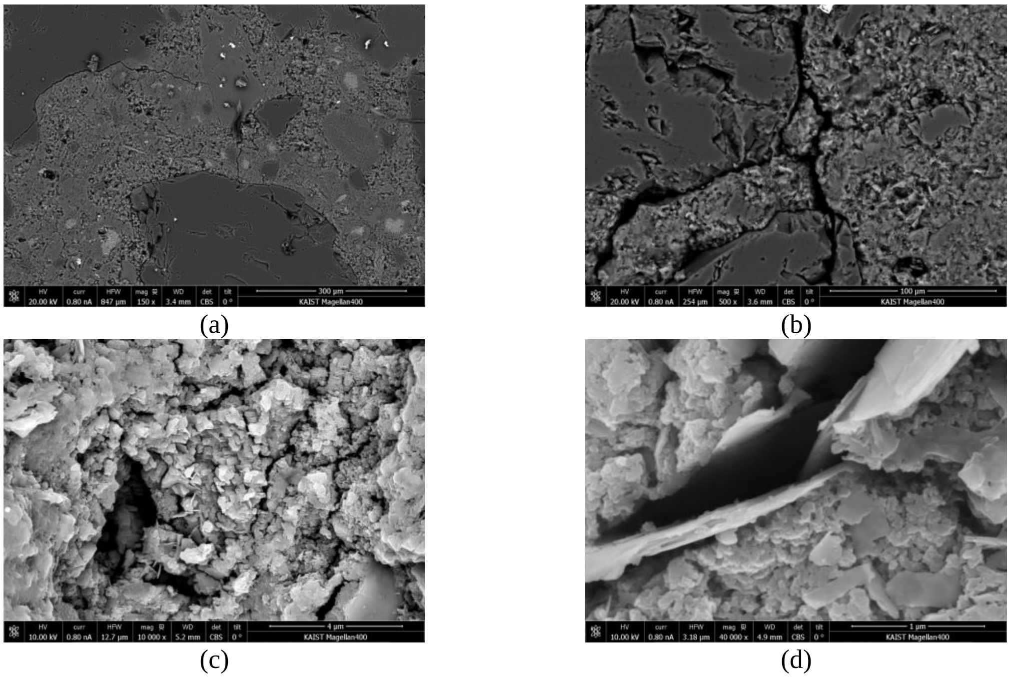


Fig. 7 SEM micrographs of damaged sample (30 F-T cycles) with magnification of (a) 150 times, (b) 500 times, (c) 10,000 times and (d) 40,000 times

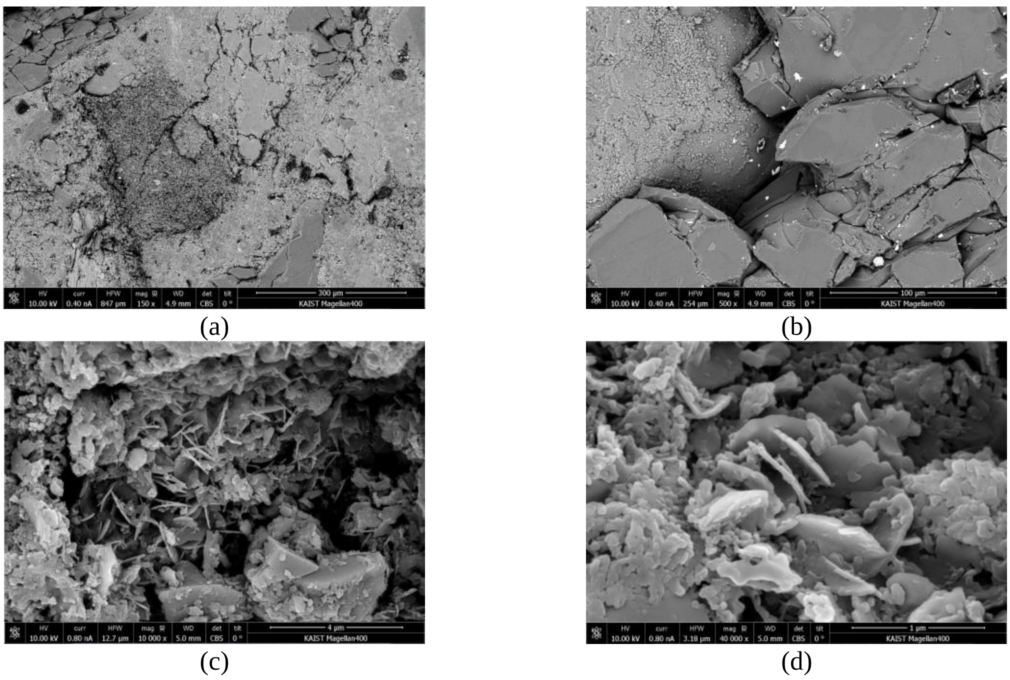


Fig. 8 SEM micrographs of damaged sample (50 F-T cycles) with magnification of (a) 150 times, (b) 500 times, (c) 10,000 times and (d) 40,000 times

In addition, the longitudinal wave velocity is determined by measuring the propagation time through a sample, which depends on the Young's modulus of the medium (ACI Committee 228 1998, ASTM C 597-09 2009). In this study, both conventional techniques were applied to all samples and the measurements were averaged for each group. The measured dynamic moduli and wave velocities are listed in Table 3. While the measured densities of each sample are approximately constant in all groups, both the dynamic modulus and the wave velocity are dependent on the elastic modulus of the samples. The elastic modulus decreased with accelerated F-T cycles. The modulus decrease appears to be caused by the increase of contact-type defects.

The sensitivity of each technique, conventional and nonlinear ultrasonic testing, was analyzed with a sensitivity parameter, where the results obtained by the conventional and nonlinear ultrasonic method are defined by $S_1(f,x)=1-(f(x)/f(0))$ and $S_2(f,x)=1-(f(0)/f(x))$, respectively (Yim *et al.* 2012a). In the definition, $f(x)$ is the $f$-measurement for the $x$-cycle sample and $f(0)$ is the $f$-measurement for an intact sample. The sensitivity parameter provides the relative variation of the experimental results with accumulated F-T damage. Converted values for all measurements represent the degree of F-T damage and are compared in Fig. 9. The highest sensitivity parameter can be found in the nonlinearity parameter measured by the impact-modulation technique, which indicates that the proposed evaluation method offers better sensitivity than the other methods. It is also attractive in the sense of allowing early detection of F-T damage.

On the other hand, ASTM C-666 (ASTM C 666-03 2008) suggests calculation of the relative dynamic modulus ($E/E_0$) of F-T damaged samples by the ratio of the decreased modulus and initial modulus. The calculated value can be converted to a durability factor to describe a failure criterion for the F-T damaged sample, where the durability index is proportional to $E/E_0$. The detailed expression can be found in ASTM C-666, but here, for example, the durability factor of sample C70 (70 F-T cycles) is 0.13 with a relative dynamic modulus of $E/E_0$=54%. The durability index vanishes if the relative dynamic modulus decreases to zero. In other words, the durability index is defined with the elastic modulus of a F-T damaged sample. Even though the elastic modulus can be correlated with the strength of concrete, the compressive strength is still the primary index to represent the material properties of concrete and its degradation. In this study, to describe the durability index the authors attempted to develop a correlation between the compressive strength and the sensitive measurement of the nonlinearity parameter.

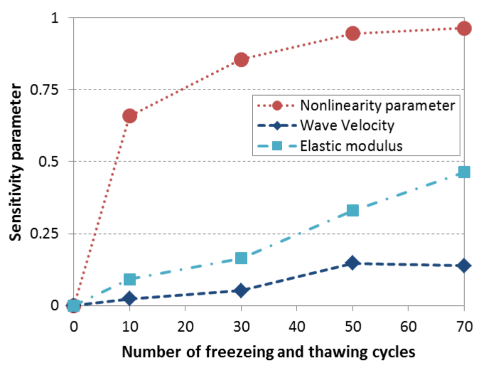


Fig. 9 Comparison of sensitivity of the conventional and nonlinear ultrasonic methods on freezing and thawing damaged concrete

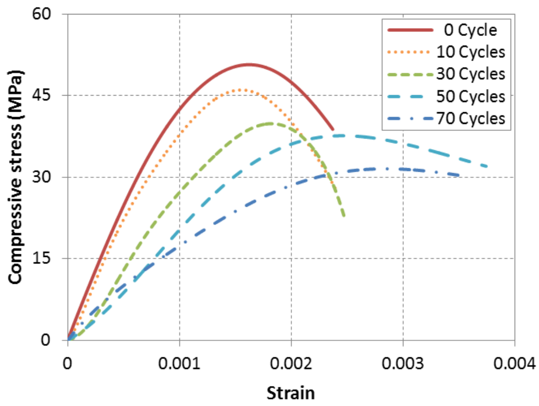


Fig. 10 Stress-strain curves of concrete samples with different freezing and thawing cycles

Fig. 10 shows uniaxial stress-strain curves of damaged samples according to different F-T cycles. Each stress-strain curve is a regression curve from averaged results of three samples. The compressive test was carried out using a universal testing machine, and the procedure to measure the compressive strength follows ASTM C-39 (ASTM C 39-01 2001). In addition, the stress-strain curve under compression was also measured with three linear variable displacement transducers mounted at one-third points along the circumference of a specimen. The compressive strength and static elastic modulus were obtained from the stress-strain curves and are listed in Table 4. Both values obviously decreased with accumulated F-T cycles. Occurrence of contact-type defects due to F-T cycles affects the compressive strength as well as the nonlinearity parameter. A correlation between the decreased ratio of compressive strength (relative compressive strength) and the increased ratio of the nonlinearity parameter was finally found, as shown in Fig. 11.

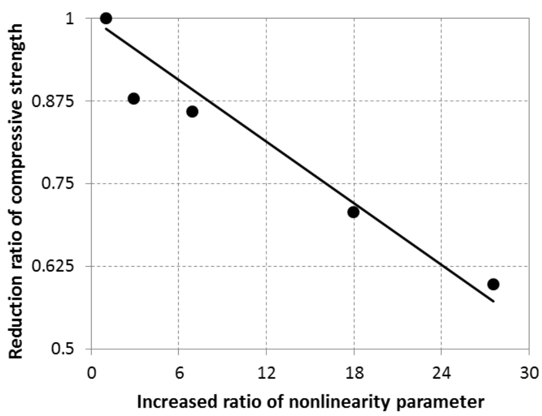


Fig. 11 Correlation between decreased ratio of compressive strength and increased ratio of nonlinearity parameter

Table 4 Compressive strength and static elastic modulus of concrete samples

| Label | Compressive strength (MPa) | Elastic modulus (GPa) |
|---|---|---|
| C00 | 50.71 | 31.79 |
| C10 | 46.06 | 31.57 |
| C30 | 39.85 | 19.20 |
| C50 | 37.63 | 13.30 |
| C70 | 31.55 | 12.28 |

## 7. Conclusions

Accumulated F-T cycles induce significant deterioration of concrete structures. This study presumed that contact-type defects are the most representative and meaningful components of F-T damage of concrete and visually verified that F-T damage consists of openings and cracks on a micro-scale. The contact-type defects are sensitive to a nonlinear parameter of the material and hence the degree of F-T damage in concrete can be assessed using this parameter. The nonlinear parameter is obtained by the impact-modulation technique, which is a nonlinear ultrasonic testing approach. Conventional tests, measurement of wave velocity (based on linear ultrasonic) and the dynamic modulus, were also accompanied to compare the sensitivity of the proposed technique. The results showed that the obtained sensitivity of the proposed technique is better than that of the conventional measurement and the suggested method is also advantageous for early detection of F-T damage of concrete. Furthermore, a correlation between the measured nonlinearity parameter and the compressive strength measured from the same samples was developed. The correlation follows a linear trend, and thus would be effective to develop a more sophisticated and comprehensive model for degradation of F-T damaged concrete.

## Acknowledgements

This research was supported by a grant(13SCIPA02) from Smart Civil Infrastructure Research Program and a grant(13SCIPA01) from Smart Civil Infrastructure Research Program funded by Ministry of Land, Infrastructure and Transport(MOLIT) of Korea government and Korea Agency for Infrastructure Technology Advancement(KAIA).

## References

ACI Committee 228 (1998), Nondestructive Test Methods for Evaluation of Concrete in Structures, America Concrete Institute, Farmington Hills, MI, USA.

Antonets, V., Donskoy, D. and Sutin, A. (1986), “Nonlinear vibro-diagnostics of flaws in multilayered structures”, *Mech. Compos. Mater.*, **15**(5), 934-937.

ASTM C 39-01 (2001), *Standard test method for compressive strength of cylindrical concrete specimens. Annual Book of ASTM Standards*, American Society for Testing and Materials (ASTM) International, West Conshohocken, PA.

ASTM C 215-08 (2008), *Standard Test Method for Fundamental Transverse, Longitudinal, and Torsional Resonant Frequencies of Concrete Specimens*, American Society for Testing and Materials (ASTM)

International, West Conshohocken, PA.

ASTM C 597-09 (2009), *Standard Test Method for Pulse Velocity Through Concrete, American Society for Testing and Materials (ASTM) International*, West Conshohocken, PA.

ASTM C 666-03 (2008), *Standard test method for resistance of concrete to rapid freezing and thawing, American Society for Testing and Materials (ASTM) International*, West Conshohocken, PA.

Buck, O., Morris, W. and Richardson, J.M. (1978), “Acoustic harmonic generation at unbonded interfaces and fatigue cracks”, *Appl. Phys. Lett*., **33**(5), 371-373.

Chen, X.J., Kim, J.Y., Kurtis, K.E., Qu, J., Shen, C.W. and Jacobs, L.J. (2008), “Characterization of progressive microcracking in Portland cement mortar using nonlinear ultrasonics”, *NDT&E Int*., **41**(2), 112-118.

Donskoy, D., Sutin, A. and Ekimov, A. (2001), “Nonlinear acoustic interaction on contact interfaces and its use for nondestructive testing”, *NDT&E Int*., **34**(4), 231-238.

Herrmann, J., Kim, J.Y., Jacobs, L.J., Qu,J., Littles, J.W. and Savage, M.F. (2006), “Assessment of material damage in a nickel-base superalloy using nonlinear Rayleigh surface waves”, *J. Appl. Phys*., **99**(12), 124913-124918.

Hikata, A., Chick, B. and Elbaum, C. (1963), “Effect of dislocations on finite amplitude ultrasonic waves in aluminum”, *Appl. Phys. Lett*., **3**(11), 195-197.

Jacobsen, S., Gran, H.C., Sellevold, E.J. and Bakke, J.A. (1995), “High strength concrete—Freeze/thaw testing and cracking”, *Cement. Concrete Res*., **25**(8), 1775-1780.

Jacobsen, S. and Sellevold, E.J. (1996), “Self healing of high strength concrete after deterioration by freeze/thaw”, *Cement. Concrete Res*., **26**(1), 55-62.

Jhang, K.Y. (2009), “Nonlinear ultrasonic techniques for nondestructive assessment of micro damage in material: a review”, *Int. J. Precis. Eng. Man*., **10**(1), 123-135.

Kim, J.H., Kwak, H.G. and Min, J. (2010), “Characterization of the crack depth in concrete using self-compensating frequency response function”, *NDT&E Int*., **43**(5), 375-384.

Kim, J.H. and Kwak, H.G. (2008), “Nondestructive evaluation of elastic properties of concrete using simulation of surface waves”, *Comput.-Aided Civil. Inf*., **23**(8), 611-624.

Mehta, P.K. and Monteiro, P.J. (2006), *Concrete: microstructure, properties, and materials* (3rd Ed.), McGraw-Hill Professional, New York, NY, USA.

Mindess, S., Young, J.F. and Darwin, D. (2003), *Concrete* (2nd Ed.), Prentice Hall, Upper Saddle River, NJ, USA.

Molero, M., Aparicio, S., Al-Assadi, G., Casati, M., Hernández, M. and Anaya, J. (2012), “Evaluation of freeze–thaw damage in concrete by ultrasonic imaging”, *NDT&E Int*., **52**, 86-94.

Nagy, P.B. (1998), “Fatigue damage assessment by nonlinear ultrasonic materials characterization”, *Ultrasonics*, **36**(1), 375-381.

Payan, C., Garnier, V. and Moysan, J. (2010a), “Effect of water saturation and porosity on the nonlinear elastic response of concrete”, *Cement Concrete. Res*., **40**(3), 473-476.

Payan, C., Garnier, V. and Moysan, J. (2010b), “Potential of nonlinear ultrasonic indicators for nondestructive testing of concrete”, *Adv. Civil. Eng*., **2010**, 1-8.

Popovics, S., Rose, J.L. and Popovics, J.S. (1990), “The behaviour of ultrasonic pulses in concrete”, *Cement Concrete. Res*., **20**(2), 259-270.

Selleck, S.F., Landis, E.N., Peterson, M.L., Shah, S.P. and Achenbach, J.D. (1998), “Ultrasonic investigation of concrete with distributed damage”, *ACI Mater. J*., **95**(1), 27-36.

Stutzman, P. (2004), “Scanning electron microscopy imaging of hydraulic cement microstructure”, *Cement Concrete Compos*., **26**(8), 957-966.

Van Den Abeele, K.E.A. (1996), “Elastic pulsed wave propagation in media with second-or higher-order nonlinearity. Part I. Theoretical framework”, *J. Acoust. Soc. Am*., **99**, 3334.

Van Den Abeele, K.E.A., Johnson, P.A. and Sutin, A. (2000), “Nonlinear elastic wave spectroscopy (NEWS) techniques to discern material damage, part I: nonlinear wave modulation spectroscopy (NWMS)”, *Res. Nondestruct. Eval*., **12**(1), 17-30.

Van Den Abeele, K.E.A., Sutin, A., Carmeliet, J. and Johnson, P.A. (2001), “Micro-damage diagnostics using nonlinear elastic wave spectroscopy (NEWS)”, *NDT&E Int*., **34**(4), 239-248.

Warnemuende, K. and Wu, H.C. (2004), “Actively modulated acoustic nondestructive evaluation of concrete”, *Cement Concrete Res*., **34**(4), 563-570.

Yang, Z., Weiss, W.J. and Olek, J. (2006), “Water transport in concrete damaged by tensile loading and freeze–thaw cycling”, *J. Mater. Civil Eng*., **18**(3), 424-434.

Yim, H.J., Kim, J.H., Park, S.J. and Kwak, H.G. (2012a), “Characterization of thermally damaged concrete using a nonlinear ultrasonic method”, *Cement Concrete Res*., **42**(11), 1438-1446.

Yim, H.J., Kwak, H.G. and Kim, J.H. (2012b), “Wave attenuation measurement technique for nondestructive evaluation of concrete”, *Nondestruct. Test. Eval*., **27**(1), 81-94.

Yim, H.J., Park, S.J., Kim, J.H. and Kwak, H.G. (2014), “Nonlinear ultrasonic method to evaluate residual mechanical properties of thermally damaged concrete”, *ACI Mater. J*., **111**(1-6), 1-11.

Zaitsev, V., Nazarov, V., Gusev, V. and Castagnede, B. (2006), “Novel nonlinear-modulation acoustic technique for crack detection”, *NDT&E Int*., **39**(3), 184-194.